2018

Molecularly imprinted artificial esterases with highly specific active sites and precisely installed catalytic groups

Lan Hu
Iowa State University

Yan Zhao
Iowa State University, zhaoy@iastate.edu

Molecularly imprinted artificial esterases with highly specific active sites and precisely installed catalytic groups

Abstract

A difficult challenge in synthetic enzymes is the creation of substrate-selective active sites with accurately positioned catalytic groups. Covalent molecular imprinting in cross-linked micelles afforded such active sites in protein-sized, water-soluble nanoparticle catalysts. Our method allowed a systematic tuning of the distance of the catalytic group to the bound substrate. The catalysts displayed enzyme-like kinetics and easily distinguished substrates with subtle structural differences.

Disciplines

Chemistry

Comments

This is a manuscript of an article published as Hu, Lan, and Yan Zhao. "Molecularly imprinted artificial esterases with highly specific active sites and precisely installed catalytic groups." *Organic & Biomolecular Chemistry* 16, no. 31 (2018): 5580-5584. DOI: 10.1039/C8OB01584H. Posted with permission.

Molecularly Imprinted Artificial Esterases with Highly Specific Active Sites and Precisely Installed Catalytic Groups

Journal:	*Organic & Biomolecular Chemistry*
Manuscript ID	OB-COM-07-2018-001584.R1
Article Type:	Communication
Date Submitted by the Author:	17-Jul-2018
Complete List of Authors:	Hu, Lan; Iowa State University, Department of Chemistry Zhao, Yan; Iowa State University, Department of Chemistry

Journal Name

COMMUNICATION

Molecularly Imprinted Artificial Esterases with Highly Specific Active Sites and Precisely Installed Catalytic Groups

Lan Hu and Yan Zhao*[a]

Received 00th January 20xx,
Accepted 00th January 20xx

DOI: 10.1039/x0xx00000x

www.rsc.org/

A difficult challenge in synthetic enzymes is the creation of substrate-selective active sites with accurately positioned catalytic groups. Covalent molecular imprinting in cross-linked micelles afforded such active sites in protein-sized, water-soluble nanoparticle catalysts. Our method allowed a systematic tuning of the distance of the catalytic group to the bound substrate. The catalysts displayed enzyme-like kinetics and easily distinguished substrates with subtle structural differences.

Enzymes routinely perform extremely challenging catalysis such as nitrogen fixation and selective C-H activation with remarkable efficiency under ambient conditions. They also tend to be highly selective among substrates with similar intrinsic chemical reactivity. The center of these feats is their active sites, where functional groups convergent from the folded peptide chain work cooperatively, sometimes with co-factors, to achieve the desired catalytic functions. In recent years, chemists have increasingly recognized the power of a functional, active-site-like microenvironment to enhance the catalyst's activity and selectivity.[1] For these biomimetic active sites, features of molecular recognition are introduced, in addition to catalytic groups, to facilitate the entry of the desire substrate over structural analogues and, in turn, to impart selectivity.

Nonetheless, in comparison to those found in enzymes, synthetic models of active sites cannot be easily tuned to accommodate substrates of different size and shape. Creation of a three-dimensional nanospace specific to a guest molecule is already a difficult challenge, let alone its multifunctionalization with molecular level precision for efficient chemical catalysis.

In this work, we report a method to introduce molecular recognition features and catalytic functionalities readily and rationally in an enzyme-resembling water-soluble nanoparticle. The work represents our continued efforts in creating biomimetic catalysts from simple building blocks.[2] The resulting artificial enzymes displayed esterase-like catalysis in the hydrolysis of activated esters and, more importantly, were able to distinguish substrates with subtle structural differences. The highlight of the method is the facile construction of the substrate-specific active site, the installment of the catalytic group at predetermined location, and the ability to fine-tune the distance of the catalytic group to the reactive group. Although hydrolysis is used as the model reaction, the method is general and should be useful in the design of other artificial enzymes with efficient and selective catalysis.

The artificial esterase was constructed through micellar imprinting developed in our laboratory.[3] Molecular imprinting[4] is a powerful technique to create guest-complementary binding sites,[5] and has been used to create synthetic catalysts for a number of reactions including hydrolysis, the Diels-Alder reaction, and aldol reactions, sometimes with remarkable activities.[4a, 6] However, several inherent challenges[7] make it difficult to manipulate imprinted active sites with molecular precision, thus limiting their usage in catalyst designs.

The synthesis of our nanoparticle catalysts is shown in Scheme 1, involving double cross-linking of the template-containing micelle of **1** (Scheme 1).[3, 8] The surface-cross-linking was achieved using diazide **2** by the click reaction and the core-cross-linking using DVB by AIBN-initiated free radical polymerization. The nanoparticles are typically decorated with sugar-derived ligand **3** for water-solubility.

The key design of our material is in the template: **4** has a methacrylate and thus will polymerize with **1** and DVB to be covalently attached to the micelle during the core cross-linking. The molecule consists of two parts: the cyan moiety is used as a photo-cleavable placeholder to introduce the catalytic pyridyl group through amine **5a–c**; the red moiety is similar to the substrate (*p*-nitrophenyl hexanoate or PNPH) in the hydrolysis. Through such a design, we can create an active site highly

[a] *Department of Chemistry, Iowa State University, Ames, Iowa 50011-3111, USA. Fax: + 1-515-294-0105; Tel: +1-515-294-5845; E-mail: zhaoy@iastate.edu.*
Electronic Supplementary Information (ESI) available: Experimental details, fluorescence titration curves, and additional figures. See DOI: 10.1039/x0xx00000x

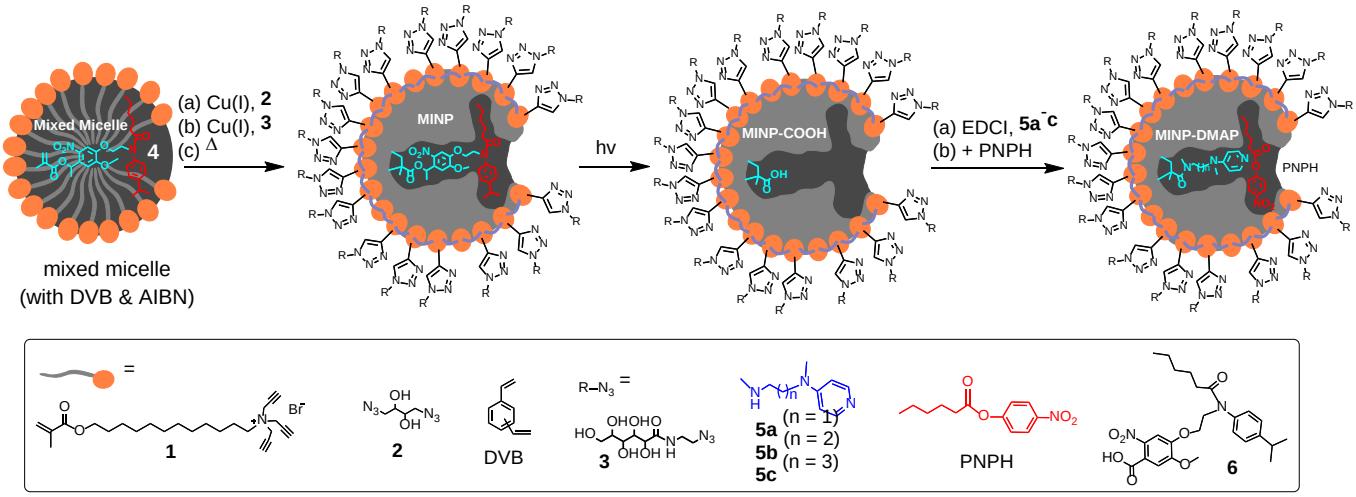

Scheme 1. Preparation of artificial esterase MINP-DMAP by micellar imprinting of template **4**.

specific to any substrate in principle, with a nearby catalytic group installed at predetermined position and angle. Compared to our earlier examples,[2c,2d] this design is expected to yield strong substrate-selectivity in the catalysis as a result of the shape-selectivity of the active site.

Synthesis and characterizations of MINPs followed published procedures.[3, 8] Generally, the surface- and core-cross-linking were monitored by ^{1}H NMR spectroscopy. The surface-cross-linking has been verified by mass spectrometry after the 1,2-diol in the cross-linked **2** was cleaved.[9] Dynamic light scattering (DSL) afforded the molecular weights of the nanoparticles and their size (~5 nm with ligand **3**). The DLS size has been confirmed by transmission electron microscopy (TEM).[10]

UV irradiation of the MINP with covalently attached **4** led to photolytic cleavage of the well-known *o*-nitrobenzyl linkage to free the template.[8b] To confirm the removal of the template,[11] we studied the binding of guest **6** by MINP-COOH, the intermediate nanoparticle to the final MINP-DMAP. We used the acid because the carboxylate was soluble enough in water for us to perform the titration. The guest is expected to fit within the binding site formed by the removal of the template due to its similarity to **4**. The carboxyl group of **6** should also hydrogen-bond with the carboxyl group of MINP-COOH through the carboxylic acid dimer.[8b] Isothermal titration calorimetry (ITC) gave an association constant of $K_a = (1.85 \pm 0.22) \times 10^4$ M^{-1} in HEPES buffer (Figure 1). The titration also revealed that the average number of the binding site per nanoparticle was N = 0.98 ± 0.06. The number agreed well with the amount of template used in the MINP preparation. Because each MINP was estimated by dynamic light scattering to have ~50 cross-linked surfactants. A 50:1 ratio of [**1**]/[**4**] is expected to afford an average of one template per nanoparticle.[3] The ITC binding thus confirmed a clean removal of the template under the photolysis condition, consistent with an earlier report.[8b]

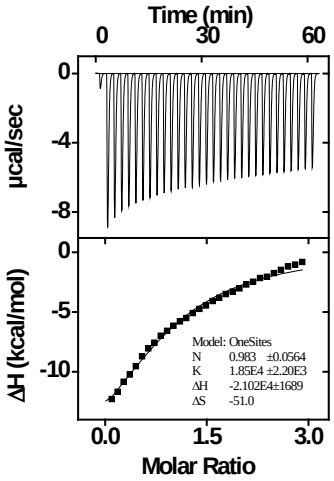

Fig 1. ITC curve obtained at 298 K from titration of MINP-COOH with **6** in 10 mM HEPES buffer (pH = 7). MINP-COOH = 80 μM in the cell. The concentration of **6** in the syringe was 1.0 mM.

MINP-COOH was then derivatized through amide coupling using EDCI. To ensure high-yielding conversion, a 10-fold excess of EDCI and the amine was used. The condition[8b] has been shown to successfully convert a carboxylic group inside the MINP pocket to the corresponding amide.[12]

The above procedures are expected to yield an active site inside the hydrophobic core of the MINP that is highly specific for binding the substrate (PNPH). The active site also contains a powerful nucleophilic catalyst (DMAP or 4,4-dimethylamino-pyridine)[13] in the proximity of the bound ester (Scheme 1). We expect the strong nucleophile would attack the ester bound in the active site, followed by the breakdown of the positively charged tetrahedral intermediate by water to regenerate the catalyst. Unlike enzymes that can only use biologically available nucleophiles, our synthetic catalysts can use more powerful groups such as DMAP. Template **4** was designed so that the pyridyl nitrogen would point to the carbonyl for the intended nucleophilic catalysis. By changing the length of the tether (n = 1–3) in the amine (**5a–c**), we can tune the distance of the catalytic pyridyl to the substrate bound in the active site. Product inhibition is not a concern because the products

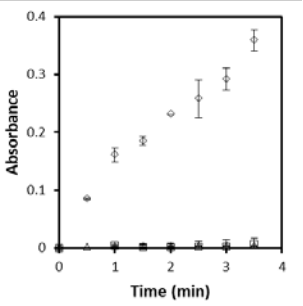

Fig 2. Absorbance at 400 nm as a function of time for the hydrolysis of PNPH in a 25 mM HEPEs buffer (pH 8.0) at 40 °C. The data sets correspond to hydrolysis in the absence of catalysts (△) and catalyzed by MINP-DMAP-**5a** (◇) and DMAP(□), respectively. [PNPH] = 50 μM. [MINP-DMAP-**5a**] = [DMAP] = 15 μM.

(hexanoic acid and *p*-nitrophenol) are more hydrophilic than the substrate and should migrate into the aqueous solution.

Figure 2 shows the hydrolysis of PNPH catalyzed by MINP-DMAP-**5a** in aqueous buffer (pH 8). The reaction was monitored by the formation of *p*-nitrophenoxide with a strong absorption at 400 nm. Our experiments show that the ester hydrolyzed negligibly in pH8 buffer, with or without molecular DMAP. Protonated DMAP has a pK_a of 9.7.[13a] At lower pH, the pyridyl nitrogen is protonated and loses its catalytic activity. The high activity of MINP-DMAP-**5a** indicates that the pyridyl behaved very differently inside the cross-linked micelle. Enzymes frequently use the microenvironment of the active site to shift the pK_a of acidic/basic groups.[14] Because ionic groups are better solvated by water than hydrocarbon, it is more difficult to protonate an amine (or deprotonate a carboxylic acid) in a hydrophobic pocket. In addition, positive charges nearby are often used by enzymes to hinder the protonation of an amine. We can easily imagine both principles in operation within the positively charged MINP.

Table 1 summarizes the rate constants of the different MINPs. In addition to PNPH, we examined three other activated esters (**7**–**9**) to understand the selectivity of our catalysts as a result of the shape and hydrophobicity of the active site. As shown by entry 1, the hydrolysis of PNPH occurred in the order of MINP-DMAP-**5a** ≈ MINP-DMAP-**5b** > MINP-DMAP-**5c**. Thus, the location of the pyridyl group inside the MINP active site did

Table 1. Kinetic data for the hydrolysis of activated esters.[a]

Entry	Ester	Rate Constant $k \times 10^4$ (s^{-1})			
		MINP-DMAP(**5a**)	MINP-DMAP(**5b**)	MINP-DMAP(**5c**)	DMAP
1	PNPH	54.8 ± 0.1	56.7 ± 3.0	42.7 ± 1.8	0.50 ± 0.17
2	**7**	1.4 ± 0.1	2.0 ± 0.3	-	0.14 ± 0.01
3	**8**	2.3 ± 0.4	1.6 ± 0.4	-	0.04 ± 0.01
4	**9**	3.9 ± 0.1	2.5 ± 0.3	-	0.35 ± 0.03

[a]The reaction rates were measured in 25 mM HEPES buffer (pH 8.0) at 40 °C. The background hydrolysis of PNPH in the same buffer was very slow, with an estimated rate constant of 0.15×10^{-4} s^{-1}. [PNPH] = 50 μM. [MINP-DMAP] = 15 μM.

affect the hydrolysis, as expected. Since the active site was created from template **4**, which has an ethylene oxide tether between the substrate-like moiety and the phenyl group, we did anticipate MINP-DMAP(**5a**) or MINP-DMAP(**5b**) to be optimal for the catalysis. The butylene oxide tether in **5c** probably is too long and might have interfered with the substrate binding or catalysis (see below for additional discussion).

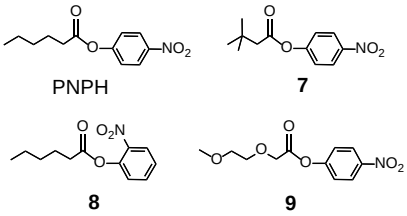

MINP-DMAP-**5a** and MINP-DMAP-**5b**, our best catalysts, both showed remarkable selectivity for the intended substrate (PNPH) over other activated ester analogues. The observed rate constants for **7**–**9** were 14–40 times slower in comparison to that of PHPH. Thus, the active site was highly selective as designed. Branching on the alkyl chain (in **7**), change of the substituent on the phenyl ring (in **8**), and an increase of hydrophilicity on the carbonyl side (in **9**) could all be distinguished with ease. In contrast, molecular DMAP in Table 1 afforded much slower kinetics and much lower selectivity in the hydrolysis—this should reflect the intrinsic reactivity of the substrate as DMAP in solution in Figure 1 gave the same reaction rates as the hydrolysis in buffer. Take PNPH and the hydrophilic **9** as the example. With molecular DMAP, the ratio of the rate constants of the two was 1.4/1 but, with MINP-DMAP-**5b**, became as high as 23/1.

All the MINPs displayed enzyme-like Michaelis–Menten kinetics described by $v_0 = V_{max}[S_0]/(K_m + [S_0])$, in which v_0 is the initial velocity, S_0 the initial substrate concentration, V_{max} the maximum velocity at a particular enzyme concentration, and K_m the Michaelis constant that measures the binding affinity of the substrate to the enzyme (ESI).[15] As shown by Table 2, MINP-DMAP-**5a** and MINP-DMAP-**5b** behaved very similarly but MINP-DMAP-**5c** was more different. The rate acceleration factor (k_{cat}/k_{uncat}) ranged from 11,000 to 17,000 for PNPH at pH8.

Earlier, we saw that MINP-DMAP-**5c** was the least active catalyst among the three for PNPH. The Michaelis-Menten study revealed that the culprit was the weak binding of the substrate, as shown by the largest K_m value of this catalyst among the three. The V_{max} and k_{cat} (= V_{max}/[enzyme concentration]) values of MINP-DMAP-**5c** were actually the highest among the three MINP catalysts.

For comparison purposes, we included data for bovine carbonic anhydrase (BCA) and α-chymotrypsin, which are frequently used in the literature to catalyze the hydrolysis of *para*-nitrophenyl esters.[16] (Note that these enzymes were not natural esterases designed to hydrolyze the activated esters). As our data shows, the MINP-DMAPs were far more active than BCA and ~40% as efficient as α-chymotrypsin, evident from the catalytic efficiency values (k_{cat}/K_m).[15] Many artificial zinc

Table 2. Michaelis-Menten parameters for the hydrolysis of PNPH catalyzed by MINP-DMAP catalysts [a] and some natural enzymes.

Entry	catalyst	V_{max} (μM/s)	K_m (μM)	k_{cat} (s^{-1})	k_{cat}/K_m ($M^{-1}s^{-1}$)
1	MINP-DMAP-**5a**	0.85±0.07	405±12	0.17±0.01	420
2	MINP-DMAP-**5b**	0.98±0.01	442±1	0.196±0.001	440
3	MINP-DMAP-**5c**	1.28±0.02	663±10	0.259±0.003	387
4	BCA	0.033±0.003	230±40	0.0042±0.0004	18
5	α-chymotrypsin	7.33±0.83	670±80	0.73±0.08	1090

[a] The reaction rates were measured in 25 mM HEPEs buffer (pH 8.0) at 40 °C in duplicates.

enzymes have been produced to mimic carbonic anhydrase and their activities were often evaluated in their catalytic hydrolysis of *p*-nitrophenyl acetate (PNPA).[17] The catalytic efficiency of our DMAP-MINPs (k_{cat}/K_m = 390–440 $M^{-1}s^{-1}$) compared favorably with the reported values (k_{cat}/K_m = 3–180 $M^{-1}s^{-1}$) for these artificial enzymes, especially considering that PNPH was less reactive than PNPA in the background hydrolysis.

Many reported synthetic esterases displayed low turnovers (10–50) in the hydrolysis of *p*-nitrophenyl esters, due to product inhibition.[17] When a large excess (500 equiv) of PNPH was used, MINP-DMAP-**5b**, our most efficient catalyst, was found to function even at high turnovers (Figure 3). The turnover number (TON) was calculated to be 390 at 600 min. The much higher turnovers observed suggest that product inhibition was much less of a problem in our catalyst than those reported in the literature.

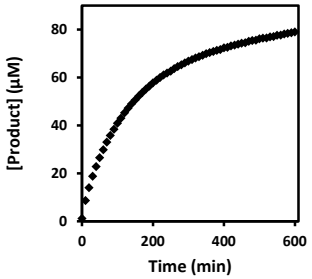

Fig 3. Amount of *p*-nitrophenoxide formed as a function of time, calculated based on an extinction coefficient of ε_{400} = 0.0216 μM^{-1} cm^{-1}. The turnover number of 390 was obtained at 600 min.

Although many artificial enzymes have been reported including ones that could hydrolyze activated esters,[1] creation of tailor-made active sites for arbitrary substrates remains a difficult challenge, making it difficult for synthetic catalysts to have high selectivity among structural analogues. The cross-linked micelle is a powerful platform to prepare strong and selective receptors for many types of molecules including small-molecule drugs,[8c] carbohydrates,[18] and peptides.[19] This work shows that the micellar imprinting method could be used rationally to create well-defined, substrate-specific active sites and accurately installed catalytic groups. A notable feature of our catalysts is the ability to fine-tune the position of the catalytic group with respect to the functional group to be transformed. This could be an extremely useful feature in the design of future artificial enzymes.

We thank NSF (We thank NSF (DMR-1464927 and CHE-1708526) for supporting this research.

Conflicts of interest

There are no conflicts to declare.

Notes and references

1. (a) M. Rakowski DuBois and D. L. DuBois, *Chem. Soc. Rev.*, 2009, **38**, 62-72. (b) J. Meeuwissen and J. N. H. Reek, *Nat Chem*, 2010, **2**, 615-621. (c) M. Raynal, P. Ballester, A. Vidal-Ferran and P. W. N. M. van Leeuwen, *Chem. Soc. Rev.*, 2014, **43**, 1734-1787. (d) O. Bistri and O. Reinaud, *Org. Biomol. Chem.*, 2015, DOI: 10.1039/C1034OB02511C.
2. (a) H. Cho, Z. Zhong and Y. Zhao, *Tetrahedron*, 2009, **65**, 7311-7316. (b) L.-C. Lee and Y. Zhao, *J. Am. Chem. Soc.*, 2014, **136**, 5579-5582. (c) G. Chadha and Y. Zhao, *Chem. Commun.*, 2014, **50**, 2718-2720. (d) L. Hu and Y. Zhao, *Helv. Chim. Acta*, 2017, **100**, e1700147.
3. J. K. Awino and Y. Zhao, *J. Am. Chem. Soc.*, 2013, **135**, 12552-12555.
4. (a) G. Wulff, *Chem. Rev.*, 2001, **102**, 1-28. (b) K. Haupt and K. Mosbach, *Chem. Rev.*, 2000, **100**, 2495-2504.
5. (a) D. Lakshmi, A. Bossi, M. J. Whitcombe, I. Chianella, S. A. Fowler, S. Subrahmanyam, E. V. Piletska and S. A. Piletsky, *Anal. Chem.*, 2009, **81**, 3576-3584. (b) T. Kuwata, A. Uchida, E. Takano, Y. Kitayama and T. Takeuchi, *Anal. Chem.*, 2015, **87**, 11784-11791. (c) J. Liu, D. Yin, S. Wang, H. Y. Chen and Z. Liu, *Angew. Chem. Int. Ed.*, 2016, **55**, 13215-13218. (d) L. Chen, X. Wang, W. Lu, X. Wu and J. Li, *Chem. Soc. Rev.*, 2016, **45**, 2137-2211. (e) R. Horikawa, H. Sunayama, Y. Kitayama, E. Takano and T. Takeuchi, *Angew. Chem. Int. Ed.*, 2016, **55**, 13023-13027. (f) M. Panagiotopoulou, Y. Salinas, S. Beyazit, S. Kunath, L. Duma, E. Prost, A. G. Mayes, M. Resmini, B. T. S. Bui and K. Haupt, *Angew. Chem. Int. Ed.*, 2016, **55**, 8244-8248. (g) D. Yin, X. Li, Y. Ma and Z. Liu, *Chem. Commun.*, 2017, **53**, 6716-6719. (h) M. Bertolla, L. Cenci, A. Anesi, E. Ambrosi, F. Tagliaro, L. Vanzetti, G. Guella and A. M. Bossi, *ACS Appl. Mater. Interfaces*, 2017, **9**, 6908-6915. (i) L. Jiang, M. E. Messing and L. Ye, *ACS Appl. Mater. Interfaces*, 2017, **9**, 8985-8995.
6. (a) G. Wulff and J. Liu, *Acc. Chem. Res.*, 2012, **45**, 239-247. (b) M. Emgenbroich and G. Wulff, *Chem.-Eur. J.*, 2003, **9**, 4106-4117. (c) S. C. Maddock, P. Pasetto and M. Resmini, *Chem. Commun.*, 2004, 536-537. (d) J.-q. Liu and G. Wulff, *J. Am. Chem. Soc.*, 2008, **130**, 8044-8054. (e) D. Carboni, K. Flavin, A. Servant, V. Gouverneur and M. Resmini, *Chem. -Eur. J.*, 2008, **14**, 7059-7065. (f) N. Kirsch, J. Hedin-Dahlström, H. Henschel, M. J. Whitcombe, S. Wikman and I. A. Nicholls, *J. Mol. Catal. B: Enzym.*, 2009, **58**, 110-117. (g) Z. Y. Chen, L. Xu, Y. Liang and M. P. Zhao, *Adv. Mater.*, 2010, **22**, 1488-1492. (h) A. Servant, K. Haupt and M. Resmini, *Chem.-Eur. J.*, 2011, **17**, 11052-11059. (i) X. Shen, C. Huang, S. Shinde, K. K. Jagadeesan, S. Ekström, E. Fritz and B. Sellergren, *ACS Appl. Mater. Interfaces*, 2016, **8**, 30484-30491. (j) A.-x. Zheng, C.-b. Gong, W.-j. Zhang, Q. Tang, H.-r. Huang, C.-f. Chow and Q. Tang, *Mol. Catal.*, 2017, **442**, 115-125. (k) C. Rossetti, M. A. Świtnicka-Plak, T. Grønhaug

Halvorsen, P. A. G. Cormack, B. Sellergren and L. Reubsaet, *Sci. Rep.*, 2017, **7**, 44298.
7. (a) S. C. Zimmerman and N. G. Lemcoff, *Chem. Commun.*, 2004, 5-14. (b) S. C. Zimmerman, M. S. Wendland, N. A. Rakow, I. Zharov and K. S. Suslick, *Nature*, 2002, **418**, 399-403.
8. (a) J. K. Awino and Y. Zhao, *Chem. Commun.*, 2014, **50**, 5752-5755. (b) J. K. Awino and Y. Zhao, *Chem.-Eur. J.*, 2015, **21**, 655-661. (c) J. K. Awino and Y. Zhao, *ACS Biomater. Sci. Eng.*, 2015, **1**, 425-430.
9. X. Li and Y. Zhao, *Langmuir*, 2012, **28**, 4152-4159.
10. (a) S. Fa and Y. Zhao, *Chem. Mater.*, 2017, **29**, 9284-9291. (b) S. Fa and Y. Zhao, *Chem. -Eur. J.*, 2018, **24**, 150-158.
11. In our previously reported MINPs, the template normally carries a polar group, often ionic, to ensure that the template would stay on the surface of the MINP. This strategy of "hydrophilic anchoring" has made it possible to remove the template by simple solvent washing. No such hydrophilic group was installed on template **4**. This is another reason why we wanted to confirm the presence of the binding site in MINP-COOH by the ITC titration of guest **6**.
12. It is difficult to know the the exact conversion yield of amidation although ITC suggested a high cleavage yield in the photolysis. For this reason, any catalytic efficiency displayed by the final MINP-DMAP should be considered the lower limit.
13. (a) G. Höfle, W. Steglich and H. Vorbrüggen, *Angew. Chem. Int. Ed. Engl.*, 1978, **17**, 569-583. (b) E. F. V. Scriven, *Chem. Soc. Rev.*, 1983, **12**, 129-161. (c) R. Murugan and E. F. V. Scriven, *Aldrichim Acta*, 2003, **36**, 21-27.
14. (a) D. Matulis and V. A. Bloomfield, *Biophys. Chem.*, 2001, **93**, 37-51. (b) J. D. Henao, Y.-W. Suh, J.-K. Lee, M. C. Kung and H. H. Kung, *J. Am. Chem. Soc.*, 2008, **130**, 16142-16143.
15. T. Palmer, *Understanding enzymes*, 4th edn., Prentice Hall/Ellis Horwood, London ; New York, 1995.
16. (a) F. J. Kezdy and M. L. Bender, *Biochemistry*, 1962, **1**, 1097-1106. (b) Y. Pocker and M. W. Beug, *Biochemistry*, 1972, **11**, 698-707. (c) L. Anoardi, R. Fornasier and U. Tonellato, *J. Chem. Soc., Perkin Trans. 2*, 1981, 260-265. (d) J. H. Harvey and D. Trauner, *Chembiochem*, 2008, **9**, 191-193.
17. (a) B. S. Der, D. R. Edwards and B. Kuhlman, *Biochemistry*, 2012, **51**, 3933-3940. (b) M. L. Zastrow, A. F. A. Peacock, J. A. Stuckey and V. L. Pecoraro, *Nat. Chem.*, 2012, **4**, 118-123. (c) M. L. Zastrow and V. L. Pecoraro, *J. Am. Chem. Soc.*, 2013, **135**, 5895-5903. (d) W. J. Song and F. A. Tezcan, *Science*, 2014, **346**, 1525-1528. (e) C. M. Rufo, Y. S. Moroz, O. V. Moroz, J. Stohr, T. A. Smith, X. Z. Hu, W. F. DeGrado and I. V. Korendovych, *Nat. Chem.*, 2014, **6**, 303-309. (f) A. J. Burton, A. R. Thomson, W. M. Dawson, R. L. Brady and D. N. Woolfson, *Nat. Chem.*, 2016, **8**, 837-844.
18. (a) J. K. Awino, R. W. Gunasekara and Y. Zhao, *J. Am. Chem. Soc.*, 2016, **138**, 9759-9762. (b) R. W. Gunasekara and Y. Zhao, *J. Am. Chem. Soc.*, 2017, **139**, 829-835.
19. J. K. Awino, R. W. Gunasekara and Y. Zhao, *J. Am. Chem. Soc.*, 2017, **139**, 2188-2191.